

OBSERVATIONS AND THE PARAMETERISATION OF AIR-SEA FLUXES DURING DIAMET

Peter A. Cook * and Ian A. Renfrew

School of Environmental Sciences, University of East Anglia, Norwich, UK

1. INTRODUCTION

1.1 The DIAMET project

DIAMET, the DIAbatic influences on Mesoscale structures in Extra-Tropical storms, is part of the UK Natural Environment Research Council (NERC) funded Storm Risk Mitigation (SRM) program. Although storms are well forecast on the synoptic-scale, the precise timing, location and morphology of the mesoscale and convective-scale structures such as strong winds and intense precipitation within these cyclones remain uncertain. So we need to parameterise key processes, such as the turbulence from the wind over the sea surface leading to an upwards flux of momentum, heat and moisture which adds to the storms, to better understand and forecast the mesoscale structure of severe storms over the UK.

In DIAMET we are using the FAAM BAe-146 aircraft in low-level flying to measure the flux of momentum, sensible heat and latent heat from the sea surface around the UK.

1.2 Air-sea fluxes

The horizontal wind at the sea surface results in shear, turbulence and vertical flux (figure 1). Early studies of air-sea interactions due to wind shear and turbulence at the sea surface, leading to fluxes of momentum, heat and moisture, were carried out by Large and Pond (1981, 1982) and by Donelan (1990). More recently Petersen and Renfrew (2009) have demonstrated the ability of the FAAM BAe-146 aircraft to produce high-quality turbulence observations (using the eddy covariance technique) at ~40 m above the sea surface during high wind speed conditions.

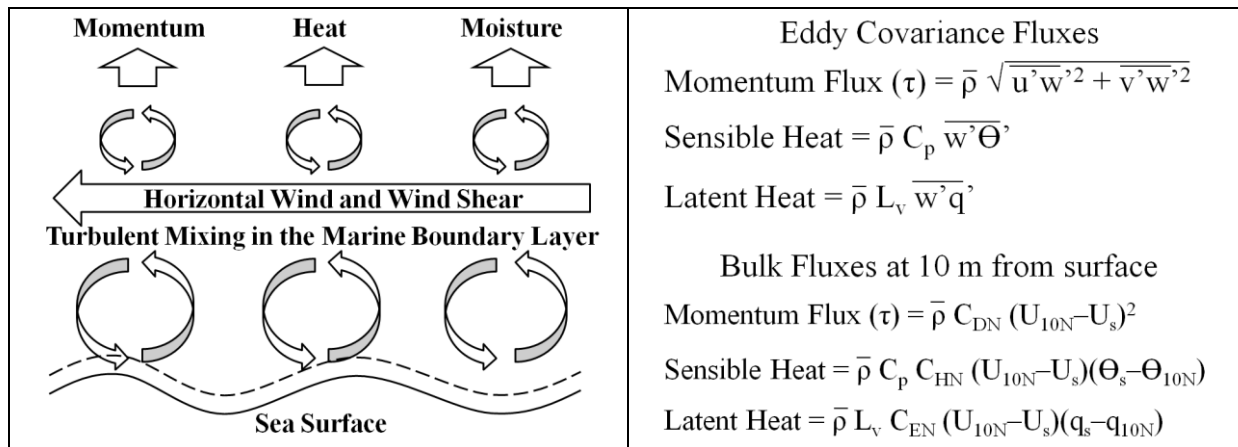


Figure 1: Turbulent fluxes due to wind shear at the sea surface, and the formulae for the eddy co-variance fluxes and the bulk fluxes.

2. THEORY

2.1 The eddy covariance technique

Aircraft are flown at low level over the sea surface in long straight legs. The turbulent fluxes of momentum, sensible heat and latent heat from the sea surface to the boundary layer are then determined from high frequency measurements of wind speed (u

* Corresponding author address: Peter A. Cook, School of Environmental Sciences, University of East Anglia, Norwich Research Park, Norwich, NR4 7TJ, UK; email: Peter.Cook@uea.ac.uk

v), updraft (w), air temperature (Θ) and humidity (q). The flight legs are divided into two minute runs (~12 km length) and within each run the products of the perturbations from the mean values are calculated ($u'w'$, $v'w'$, $w'\Theta'$ and $w'q'$). These products are used in eddy covariance to determine the fluxes (figure 1).

2.2 Bulk fluxes

However large-scale numerical weather prediction (NWP) models require parameterised bulk fluxes between the sea surface and air, which just depend on the wind speed at the 10 m neutral reference height (U_{10N}) and on the differences in temperature ($\Theta_s - \Theta_a$) and humidity ($q_s - q_a$). The formulae for the bulk fluxes contain three neutral exchange coefficients (C_{DN} , C_{HN} and C_{EN}) which need to be determined (figure 1).

3. AIRCRAFT MEASUREMENTS

3.1 The BAe-146

In DIAMET we are using aircraft measurements to determine the air-sea fluxes. The Facility for Airborne

Atmospheric Measurements (FAAM) uses a specially built BAe-146 to provide a very versatile platform for instruments, it is operated by the UK Met Office and the National Centre for Atmospheric Science (NCAS) on behalf of NERC, and has been used in many field campaigns around the world since 2004 (figure 2). The aircraft is able to fly down to only 30-40 m above the sea surface, and here measure the low level winds, updrafts, air pressure, temperature and humidity, and also the sea surface temperature.

3.2 Why an aircraft?

But why use an aircraft to measure low level winds, sea surface temperature and air-sea fluxes rather than a ship? With an aircraft we have a platform that is independent of the sea surface, giving less distortion of the airflow, able to cover larger areas, and can quickly reach and investigate areas with interesting meteorology. Although with an aircraft we obtain lower resolution data, require more quality control of the data and have limited time of operation.

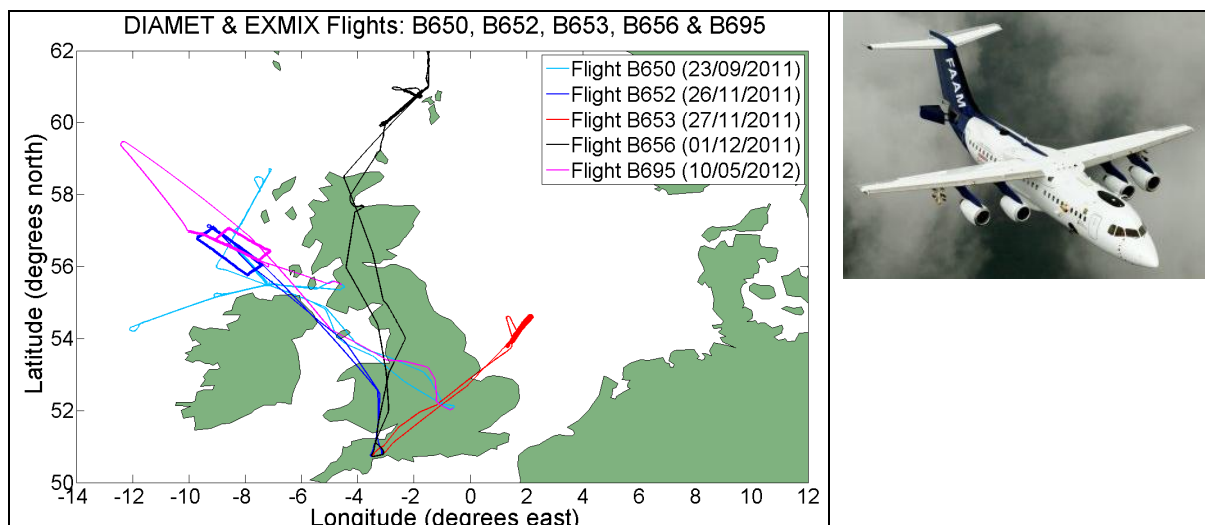


Figure 2: The FAAM BAe-146, and the five flight paths with low-level legs during DIAMET. Though B653 is counted as a Met Office EXMIX flight.

4. THE DATA COLLECTED AND USED

4.1 The 5 DIAMET flights

For DIAMET the BAe-146 has so far been used in three flying campaigns: from Cranfield, Bedfordshire, in September 2011, from Exeter, Devon, in November and December 2011, and from Cranfield in May 2012.

Low level measurements have been obtained from 5 flights (figure 2), divided into a total of 151 straight line runs of 2 minute length (~12 km). In each low-level run the fluxes of momentum (wind stress), sensible heat and latent heat can be calculated from the high frequency measurements by using the eddy covariance technique. Although many of the runs contain mesoscale features and not pure turbulence,

and these need to be left aside as poor quality data since any calculations would lead to inaccurate turbulent fluxes.

4.2 The 19 further flights

Measurements from a further 19 flights with low-level legs over the sea have also been used in this study, mostly from around the UK, and the same calculations and quality control were applied.

5. INSTRUMENTATION

5.1 In-situ instruments

Wind speed (u, v), updraft (w) and air pressure (p) are measured by a Five-Port Pressure Measurement System at 32 Hz (giving a spatial resolution of ~ 3 m). Air temperature (Θ) is measured by a Rosemount Sensor at 32 Hz, and air humidity (q) by a Lyman Alpha Hygrometer at 64 Hz.

5.2 Remote sensing of surface temperature

However the sea surface temperature (SST) has to be measured remotely which is more difficult. During each flight a Heimann Radiometer is used (at 4 Hz), though at present there are some questions over its calibration, the corrected values can be less accurate than the uncorrected values. So many of the flights (but not all) also used an interferometer (ARIES) to make limited SST measurements and so check the Heimann.

5.3 Use of OSTIA satellite data

Because of this difficulty for each flight we use independent SST measurements from OSTIA – the Operational Sea Surface Temperature and Sea Ice Analysis, Donlon et al. (2011). The OSTIA values at noon on the date of the flight at many regularly spaced locations are interpolated to the aircraft position for every second of low level flight. For the calculations in this study we use uncorrected Heimann values which are offset so that they coincide with OSTIA values at low levels. The humidity of the air at sea surface is calculated from the temperature by assuming 98% saturated relative humidity (for salt water).

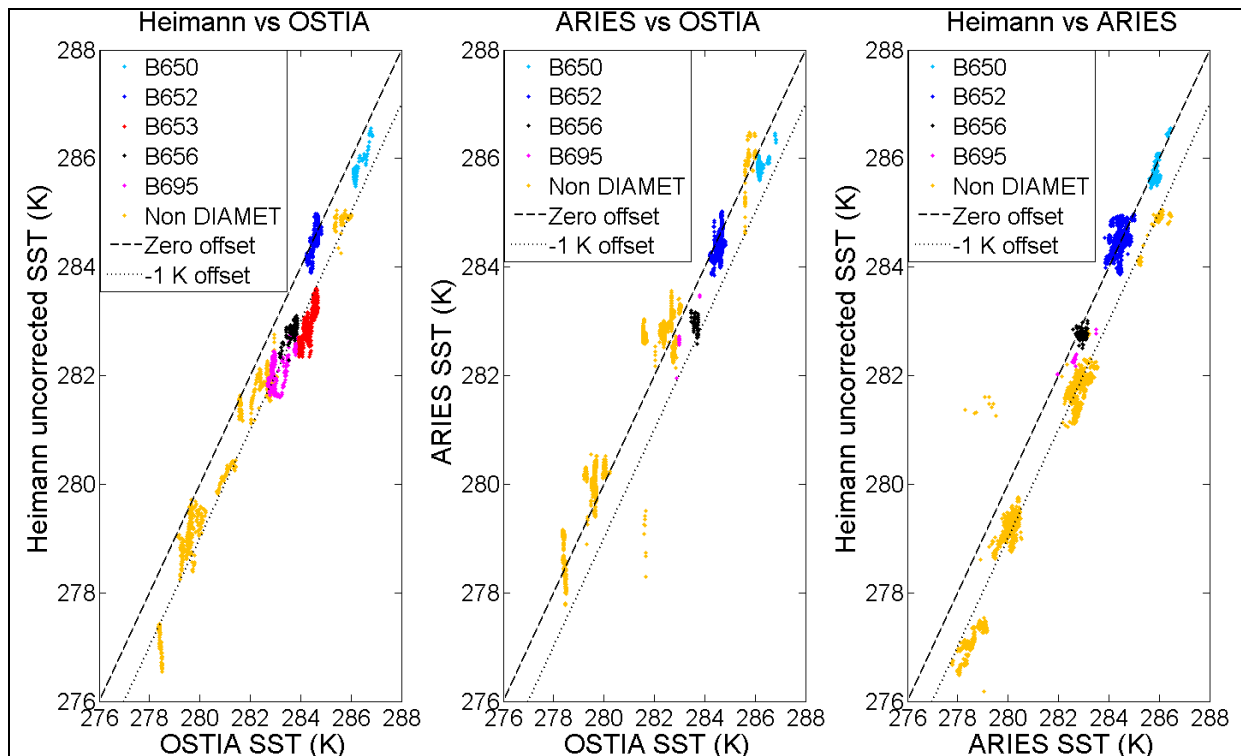


Figure 3: Scatter plots comparing the 3 sets of sea surface temperature values, from 13 flights.

OSTIA website: http://ghrsst-pp.metoffice.com/pages/latest_analysis/ostia.html

5.4 Comparing the temperature measurements

We need to determine the best sea-surface temperature (SST) measurements during each flight because the values of C_{HN} and C_{EN} strongly depend on these. The 3 sets of SST measurements are in good agreement for some flights (e.g. B650 and B652), for others the ARIES and OSTIA are in good agreement but uncorrected Heimann values are lower by around 1.0 K (e.g. B656 and B695). This gives confidence in the ARIES and OSTIA values. The SST measurements from 13 flights are compared in figure 3 (there were no ARIES measurements during flight B653). Since the OSTIA values are typically larger than the uncorrected Heimann, by more than 1.0 K for some flights, using the OSTIA values in the calculations results in significantly smaller values for the C_{HN} and C_{EN} neutral exchange coefficients.

6. USING THE DATA

6.1 Quality control

The data and co-variances are put through a complex quality control to find the runs which contain pure turbulence, and any runs which also contain larger mesoscale features (100's of metres wide) are left aside. First basic power spectra are taken of both the data (u , v , w , Θ , q) and the covariances ($u'w'$, $v'w'$, $w'\Theta'$ and $w'q'$) within each run, and these should have a $-5/3$ gradient if there is just turbulence.

Then cumulative summations of the covariances over each run are examined, and these will be close to a straight line if there are no large mesoscale features.

Finally the co-spectra of the covariances are calculated, and these should have almost zero variation at low frequencies (~ 1 Hz), and cumulative summations of the co-spectra should show a smooth curve. The quality control process is detailed in Petersen and Renfrew (2009).

6.2 Calculation of the coefficients

All the calculations used to find the wind speed (U_{10N}) and the three exchange coefficients (C_{DN} , C_{HN} and C_{EN}) at the 10 m neutral reference height, from

the aircraft measurements and the eddy covariances, are detailed in Petersen and Renfrew (2009). These include a correction for the friction velocity at the surface due to the Coriolis force, Donelan (1990), and empirical stability functions to account for the boundary layer stability, Paulson (1970) for unstable conditions.

7. RESULTS

7.1 The calculated values

The preliminary results from the measurements are over a range of wind speeds 7 – 24 m/s (U_{10N} at 10 m), and have a range of calculated wind stresses 0 – 3 N/m², sensible heat fluxes -40 – 280 W/m², and latent heat fluxes -60 – 570 W/m². The instrumentation produces measurement errors in the wind speed, updraft, temperature and humidity. These errors are combined according to the bulk formulae to determine the errors on the neutral exchange coefficients.

7.2 Plotting the fluxes

The plots of wind stress (τ) vs U_{10N}^2 , sensible heat flux (SH) vs $U_{10N}*(\Theta_s - \Theta_a)$, and latent heat flux (LH) vs $U_{10N}*(q_s - q_a)$ from the five flights show roughly linear relationships, supporting the bulk flux equations (figures 4-6). The dashed lines on the figures show constant coefficient values of 0.001 and 0.002.

7.3 Plotting the coefficients

However the neutral exchange coefficients actually depend on the wind speed U_{10N} and plotting the calculated values of C_{DN} , C_{HN} and C_{EN} reveals the different dependences. Here the values from the five DIAMET flights are plotted with the values calculated from nineteen other flights which had low level legs (figures 7-9). C_{DN} is seen to increase sharply with U_{10N} , but C_{HN} and C_{EN} show only small increases with U_{10N} .

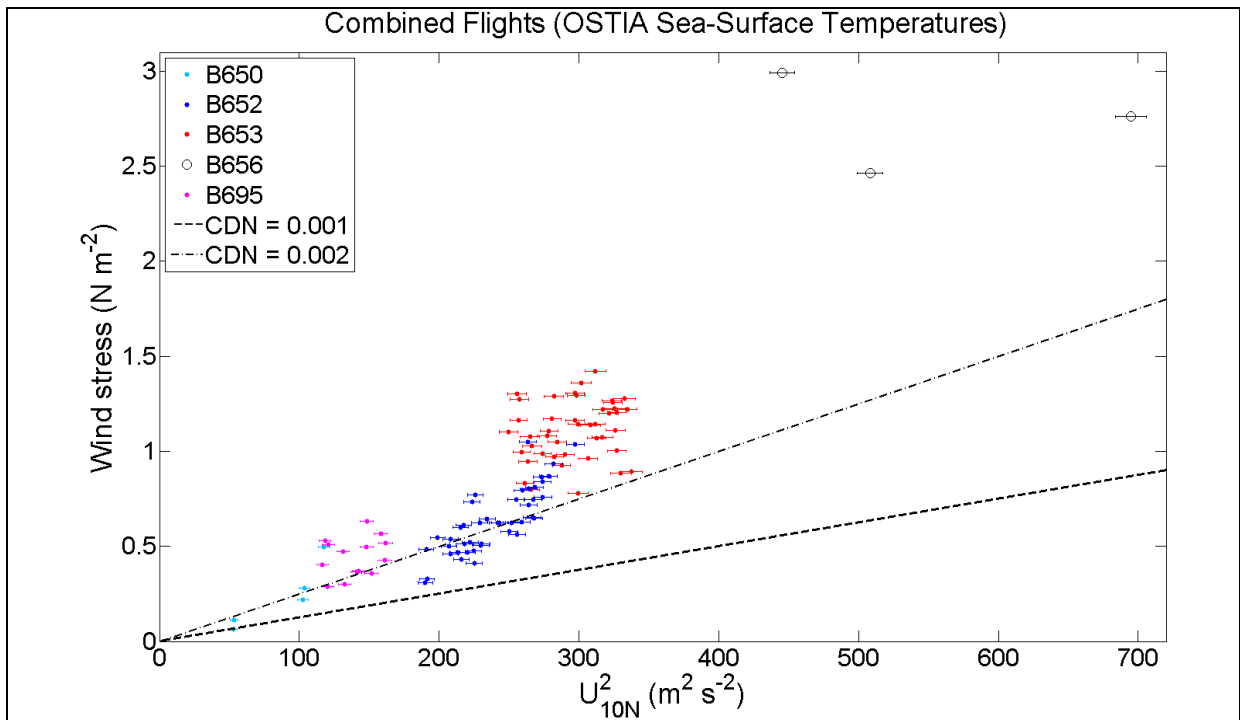


Figure 4: The momentum flux (wind stress) values from the low-level runs calculated by eddy co-variance.

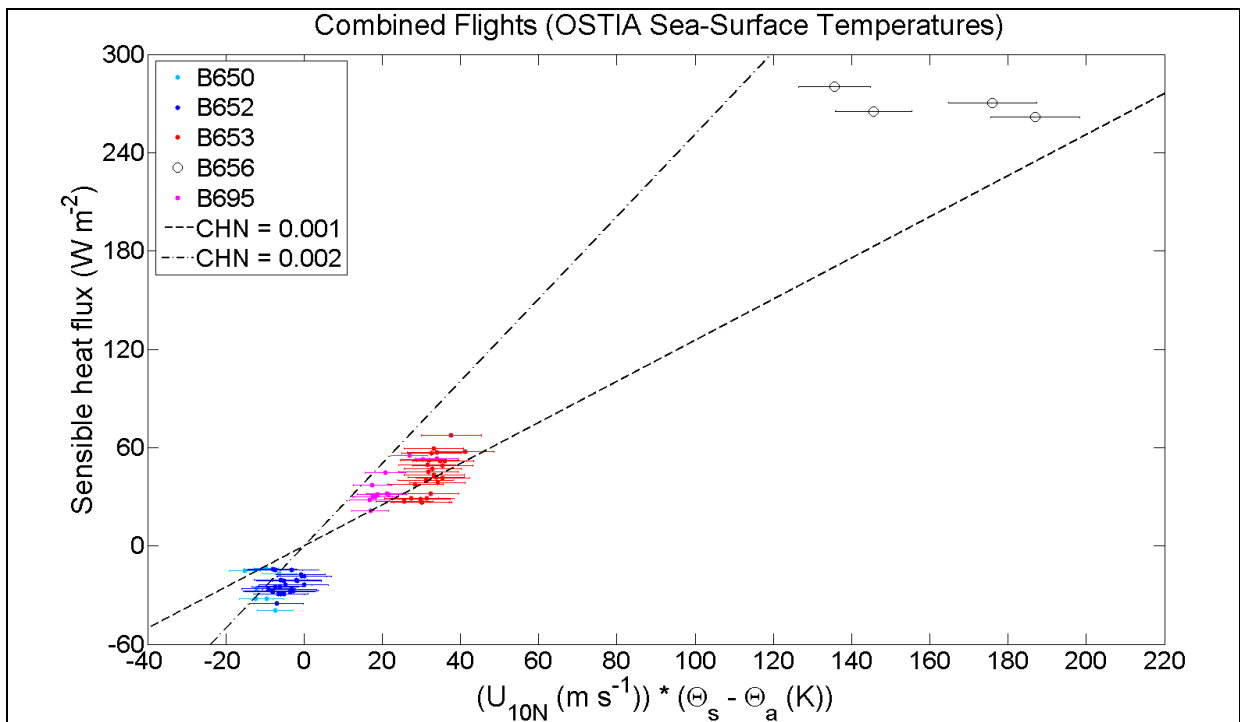


Figure 5: The sensible heat flux values from the low-level runs calculated by eddy co-variance.

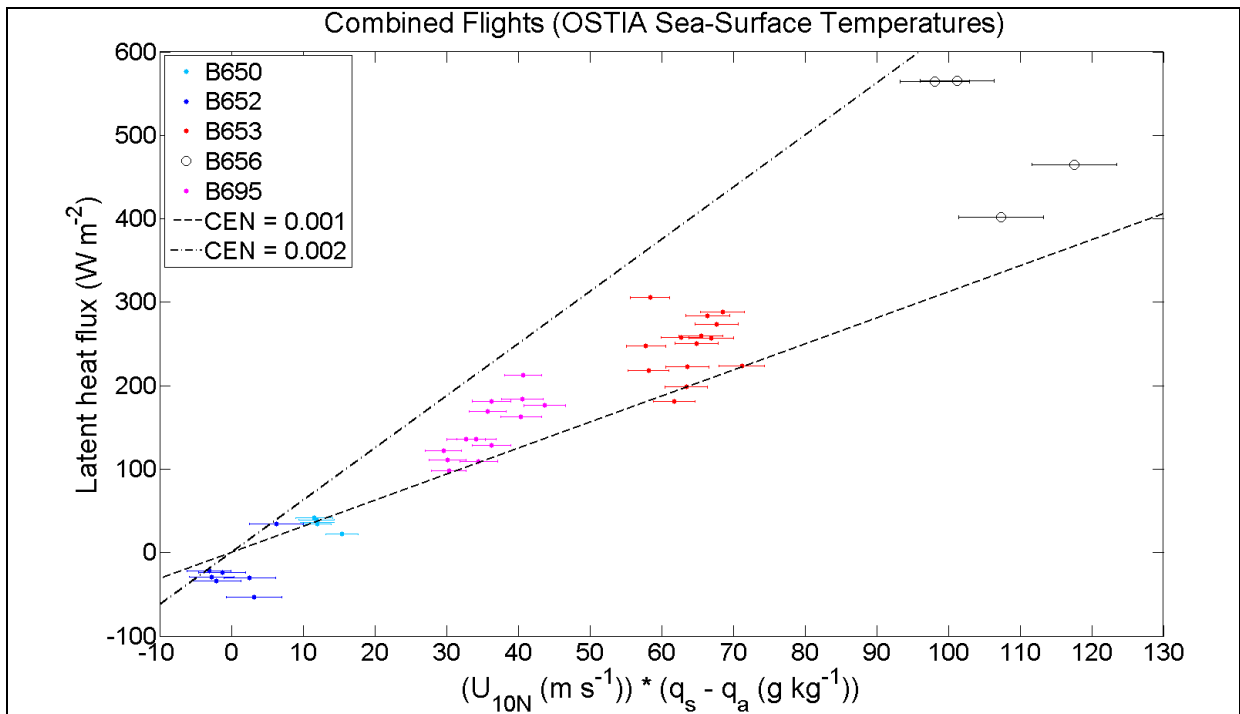


Figure 6: The latent heat flux values from the low-level runs calculated by eddy co-variance.

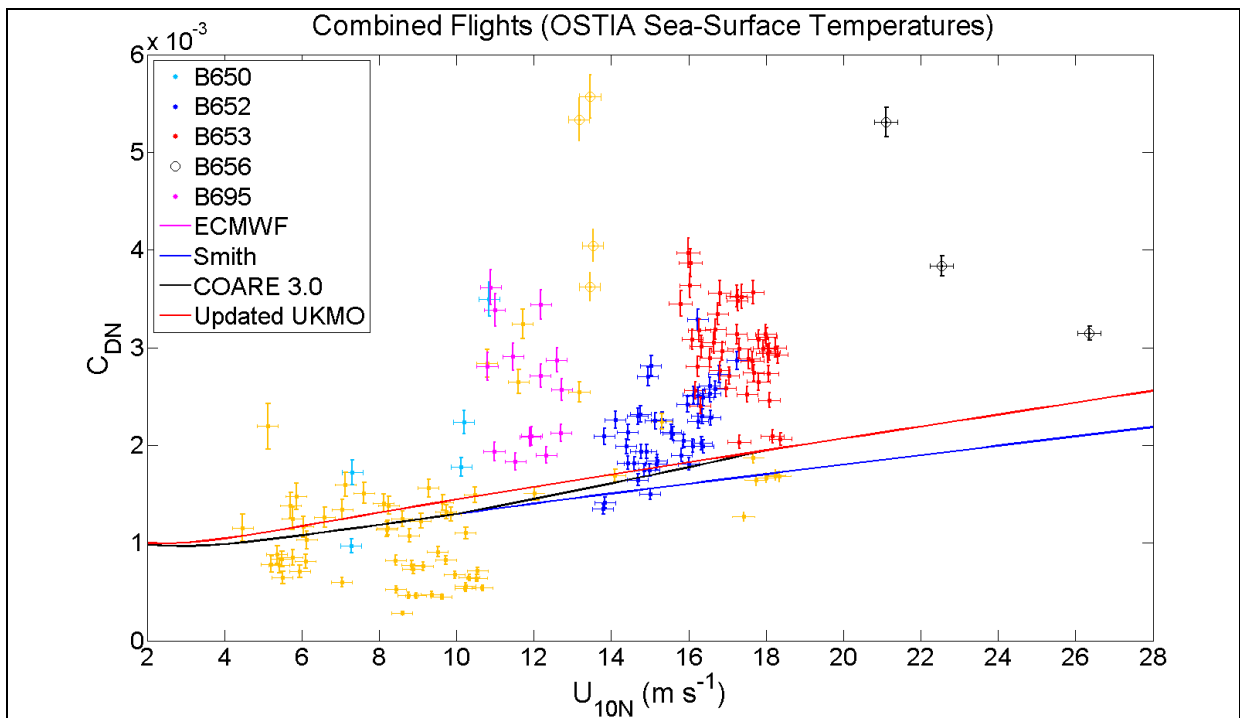


Figure 7: Momentum flux coefficient vs wind speed at the neutral reference height, low-level runs from many flights, with the previously developed algorithms marked on. Values marked by O are from flights where the boundary layer was very unstable, such as B656.

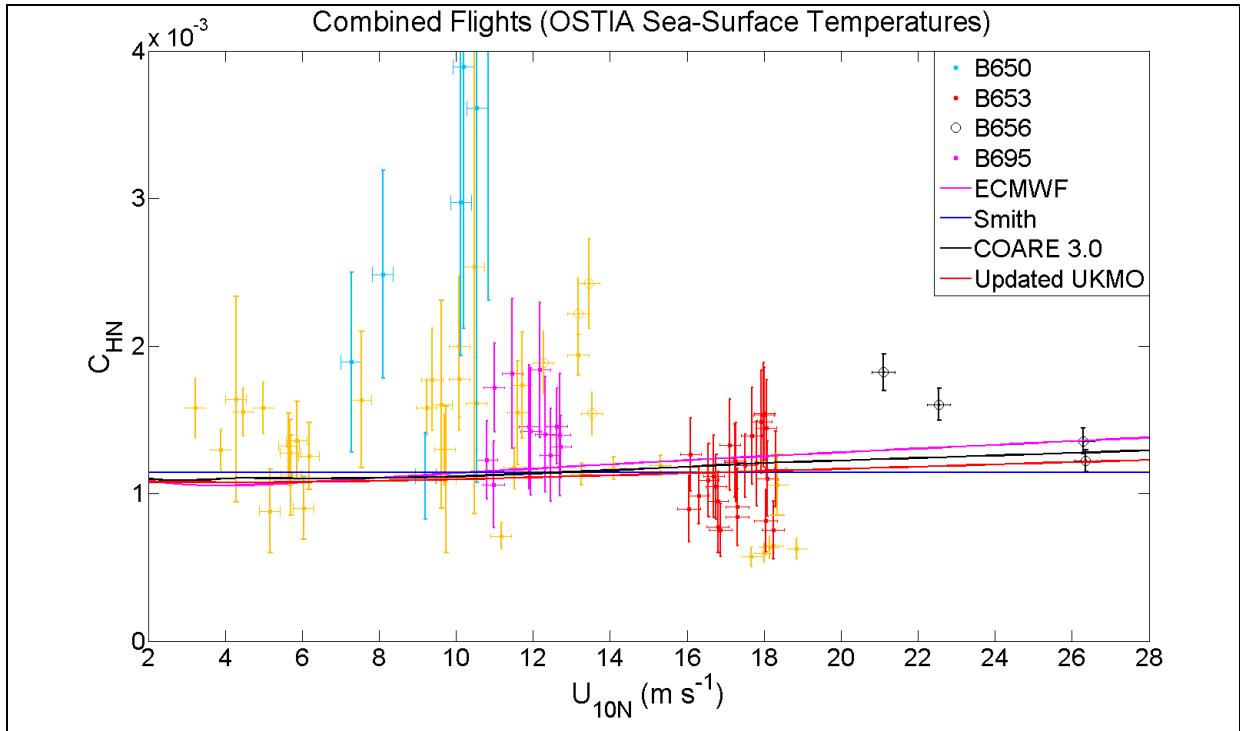


Figure 8: Sensible heat flux coefficient vs wind speed at the neutral reference height, low-level runs from many flights, with the previously developed algorithms marked on. The values from flights where θ_s and θ_a are very similar, such as B652, have very large errors and so are excluded here.

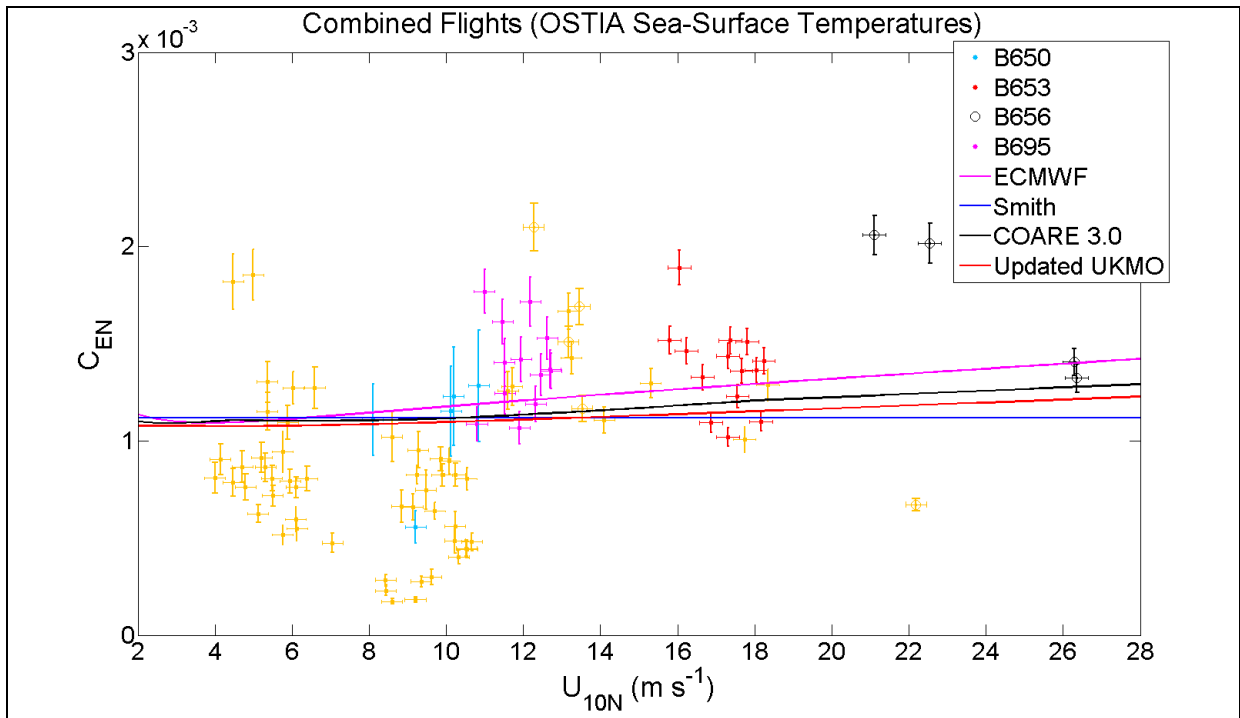


Figure 9: Latent heat flux coefficient vs wind speed at the neutral reference height, low-level runs from many flights, with the previously developed algorithms marked on. The values from flights where q_s and q_a are very similar, such as B652, have very large errors and so are excluded here.

7.4 Comparison to previous algorithms

There have been a number of previous studies of air-sea fluxes and different groups have developed their own bulk flux algorithms for how the three neutral exchange coefficients depend on wind speed. However the measurements of fluxes are still limited in number, particularly at large wind speeds where the coefficients increase so that the fluxes have a non-linear response to the wind. So there remains considerable uncertainty in the parameterisations of the air-sea fluxes, and the good quality fluxes calculated here can be used to develop and validate new bulk flux parameterisation algorithms.

Hence figures 7-9 also show the algorithms for C_{DN} , C_{HN} and C_{EN} that have been developed and used by the European Centre for medium range weather forecasts (ECMWF), Smith (Smith 1988), COARE 3.0 (Fairall 2003), and the UK Met Office (UKMO).

The new coefficient values calculated from the DIAMET measurements are clearly greater at large wind speeds ($U_{10N} > 10$ m/s) than the previously developed algorithms, many C_{DN} values by around 50% and many C_{HN} and C_{EN} values by around 20%. Although using the OSTIA SST values instead of the uncorrected Heimann measurements has reduced the C_{HN} and C_{EN} values.

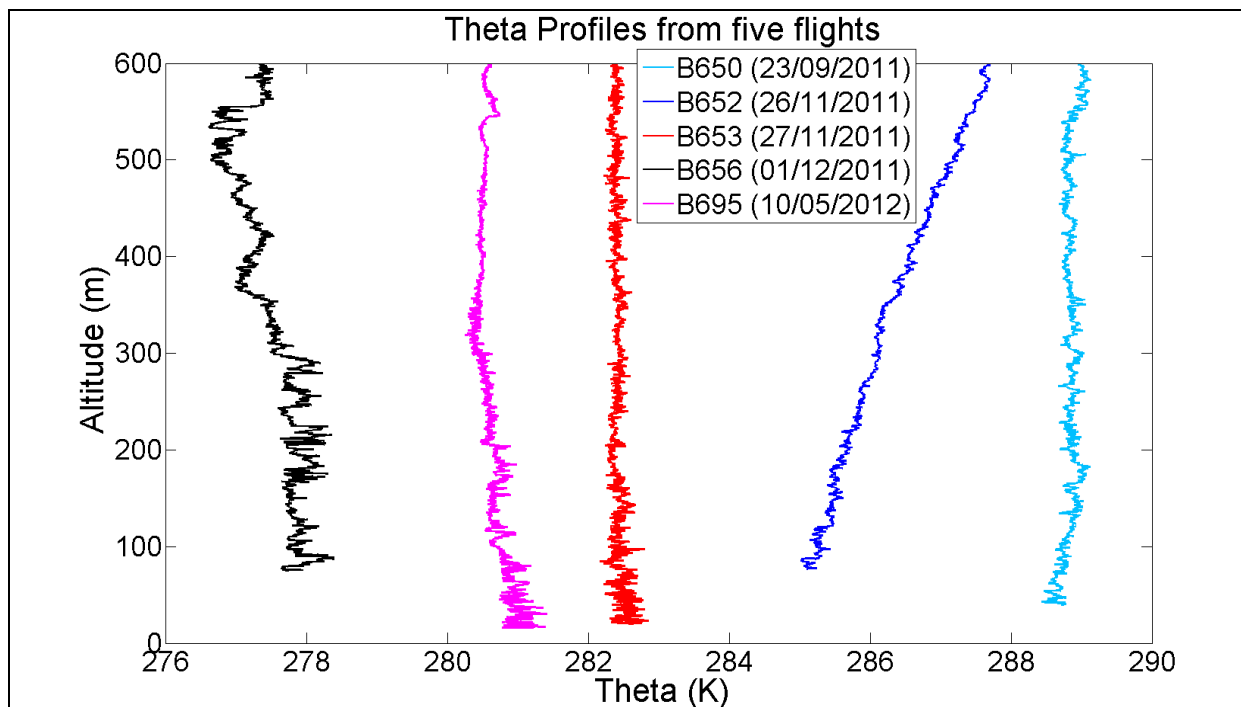


Figure 10: Measured theta profiles from the 5 DIAMET flights.

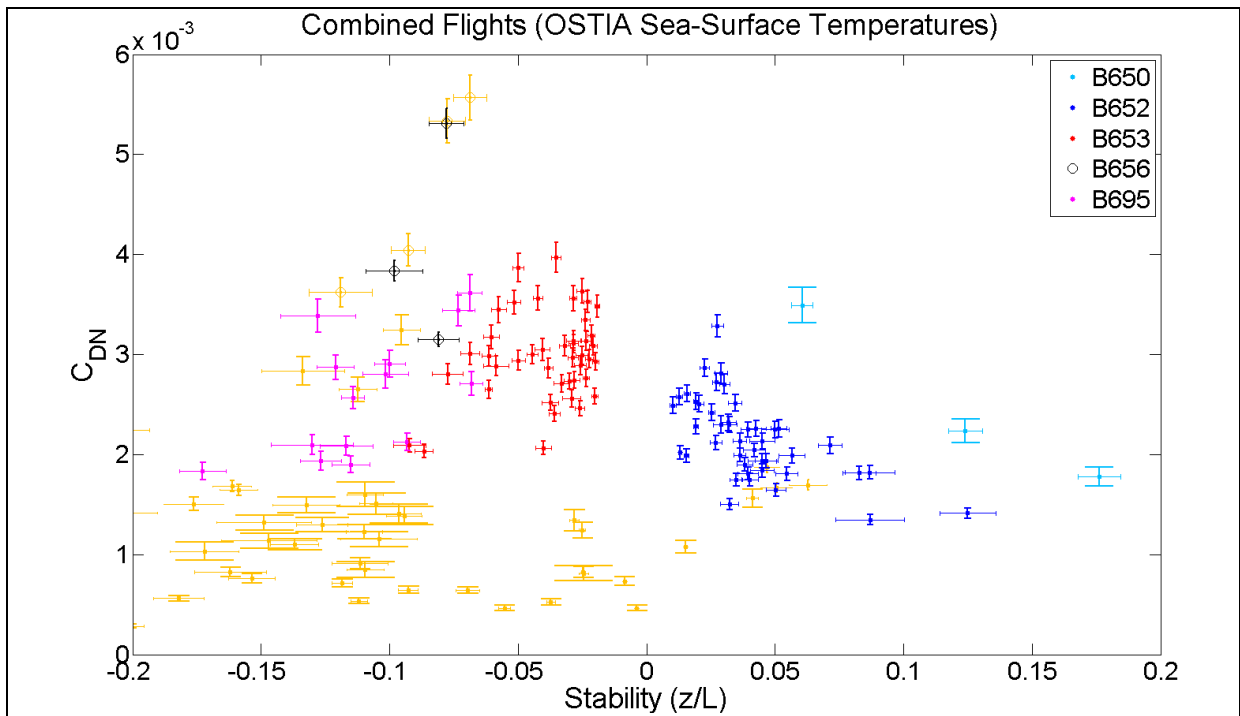


Figure 11: Momentum flux coefficient vs stability, low-level runs from many flights.

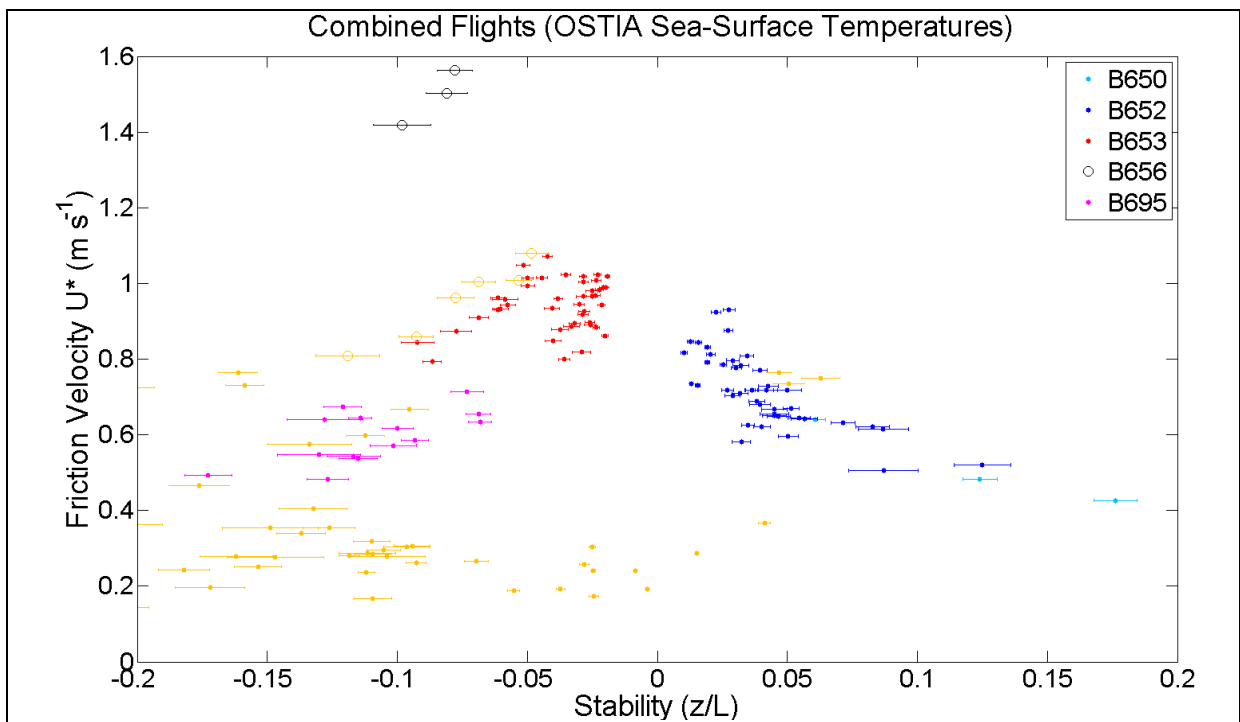


Figure 12: Friction velocity (from covariances $u'w'$ and $v'w'$) vs stability, low-level runs from many flights.

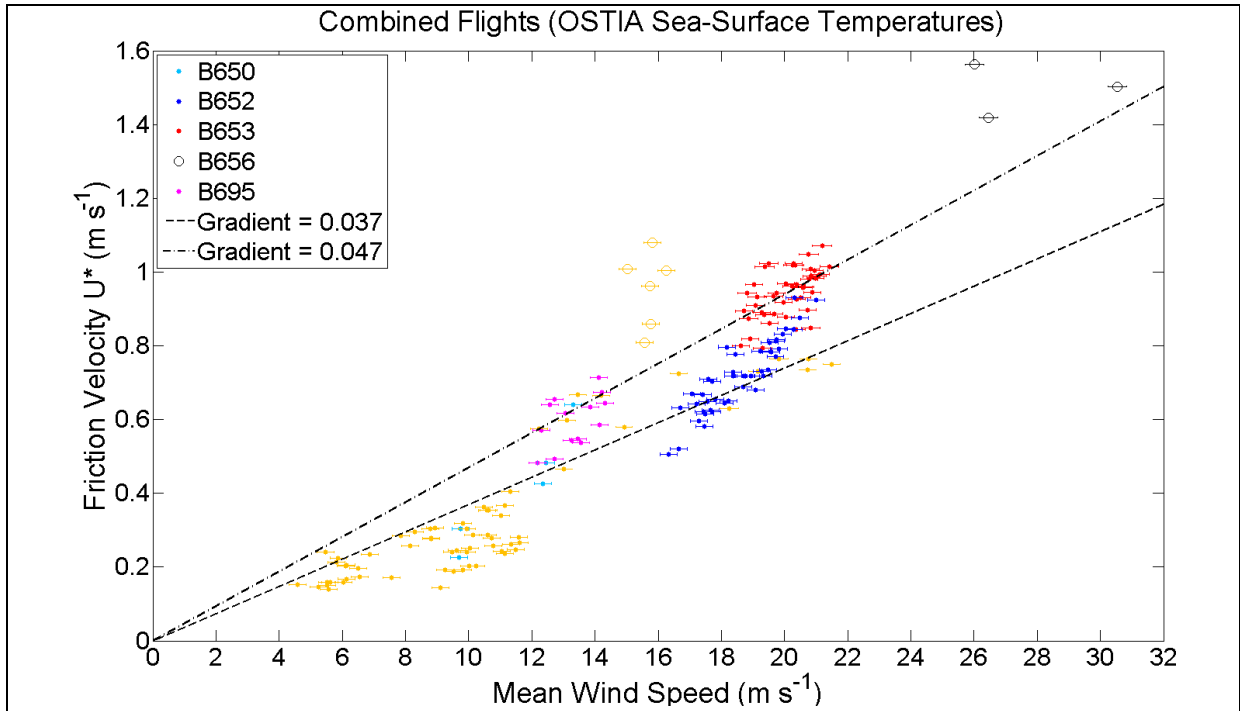


Figure 13: Friction velocity vs mean wind speed, low-level runs from many flights.

7.5 Stability of the boundary layer

However some of the C_{DN} values are very large (figure 7), particularly from flight B656 and one of the other flights, and this seems to be due to unstable boundary layers, even though empirical stability functions have been applied in the calculations. Figure 10 shows the measured theta profiles from the five DIAMET flights, B650 and B652 had stable boundary layers where theta increases with altitude, while the other flights were in unstable boundary layers. Figure 11 plots C_{DN} against the air stability at the flight level (z/L), and the values are clearly greater within unstable air. There is still a dependence on air stability after the empirical stability functions have been applied.

Unstable boundary layers probably set up additional turbulence which adds to the turbulence from the wind shear at the sea surface. Figure 12 plots the friction velocity U^* (calculated from the covariances $u'w'$ and $v'w'$) against the air stability at flight level (z/L), and this is also clearly greater within unstable air. Though since the friction velocity also depends on the mean wind speed, the friction velocity is also plotted against wind speed (figure 13). The flights within unstable boundary layers measure greater friction velocities at similar wind speeds than the other flights, following a steeper gradient and implying that there was additional turbulence.

8. Conclusions

The recent DIAMET flights have gone well and some good quality measurements have been obtained at low levels in a variety of wind speeds. These results, along with the data from many other flights, will be useful for the development and validation of bulk flux algorithms and potentially testing coupled Numerical Weather Prediction models. Although quality control is required to find the low level runs containing pure turbulence and no mesoscale features.

We are still determining the best sea surface temperature (SST) measurements to use in the calculations, since for many of the flights the OSTIA SST values are significantly greater than the uncorrected Heimann radiometer measurements. However the limited SST measurements from the ARIES interferometer support the OSTIA values. Using the OSTIA SST values the coefficients C_{HN} and C_{EN} are reduced, but these are still ~20% greater than in the algorithms developed in previous studies at large wind speeds ($U_{10N} > 10$ m/s).

Many of the C_{DN} coefficients are ~50% greater at large wind speeds ($U_{10N} > 10$ m/s) than in the previously developed algorithms. However the flights which have produced the largest values took place in unstable boundary layers, and here vertical mixing

seems to have added further turbulence to that from the wind shear at the sea surface. An increase in the friction velocity U^* of 15% would lead to a 50% increase in the calculated values of C_{DN} .

We will go onto collaborate with the DIAMET partners on validation of the Met Office Unified Model, and in further investigation of particular cases.

9. Acknowledgements

We wish to thank NERC for funding DIAMET through the Storm Risk Mitigation program, and FAAM for flying the BAe-146 and providing the detailed measurements.

10. References

- Donelan, M. A., 1990: Air-sea interaction. *The Sea*, Wiley-Interscience, New York, 239-292.
- Donlon, C. J., et al., 2011: The Operational Sea Surface Temperature and Sea Ice Analysis (OSTIA). *Remote Sensing of the Environment*, doi: 10.1016/j.res.2010.10.017.
- Fairall, C. W., et al., 2003: Bulk parameterization of air-sea fluxes: Updates and verification for the COARE algorithm. *J. Climate*, 16, 571-591.
- Large, W. G., and Pond, S., 1981: Open ocean momentum flux measurements in moderate to strong winds. *J. Phys. Oceanogr.*, 11, 324-336.
- Large, W. G., and Pond, S., 1982: Sensible and latent heat flux measurements over the ocean. *J. Phys. Oceanogr.*, 12, 464-482.
- Paulson, C. A., 1970: The mathematical representation of wind speed and temperature in the unstable atmospheric boundary layer. *J. Appl. Meteorol.*, 9, 857-861.
- Petersen, G. N., and Renfrew, I. A., 2009: Aircraft-based observations of air-sea fluxes over Denmark Strait and the Irminger Sea during high wind speed conditions. *Q. J. R. Meteorol. Soc.*, 135, 2030-2045.
- Smith, S. D., 1988: Coefficients for sea surface wind stress, heat flux and wind profiles as a function of wind speed and temperature. *J. Geophys. Res.*, 93, 15467-15472.